ELASTIC WAVE SCATTERING BY GENERAL SHAPED DEFECTS: THE DISTORTED WAVE BORN APPROXIMATION

E. Domany,[a] K.E. Newman and S. Teitel[b]
Department of Physics, University of Washington
Seattle, Washington 98195

ABSTRACT

An approximate theory for scattering of elastic wave by general shaped defects has been developed. A defect of arbitrary shape can be represented by a sphere S and a remainder volume R. Using the exact solution for a sphere and treating R as a perturbation, the solution corresponding to the Distorted Wave Born Approximation is obtained. This solution contains non-trivial frequency dependence and phase information. Preliminary comparisons with experiments will be presented.

INTRODUCTION

Development of reliable approximation methods to elastic wave scattering by defects is an important part of NDE research. We have recently introduced the Distorted Wave Born Approximation,[1] to study scattering by defects of quite general shape. This method is expected to yield nontrivial phase information and frequency dependence of the scattered fields. Such information is of importance for development of inversion procedures, and for selecting an optimal set of measurements needed to characterize the defect.

The relative advantages of the DWBA were presented in a previous communication,[1] where the basic definitions and formulae were also given. In what follows we present a brief summary of the formalism and proceed to the new, final results.

THE DISTORTED WAVE BORN APPROXIMATION-- REVIEW OF FORMALISM

The DWBA starts by representing a general shaped defect R as a spherical region S and a remainder $\bar{R}$ (see Fig. 1). The exact solution of the scattering equation satisfies the integral equation[1]

$$u_i(\underline{r}) = u_i^S(\underline{r}) + \delta\rho\omega^2\int_{\bar{R}} d\underline{r}' g_{im}^S(\underline{r},\underline{r}')u_m(\underline{r}') - \delta C_{jklm}\int_{\bar{R}} d\underline{r}' g_{ij,k'}^S(\underline{r},\underline{r}')u_{l,m'}(\underline{r}') \quad , \quad (1)$$

$$R = S + \bar{R}$$

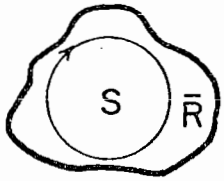

Fig. 1. The defect R is represented as a sphere S and a "remainder" volume $\bar{R}$.

where u_i^S is the solution to the scattering problem by the sphere S, and $g_{ij}^S(\underline{r},\underline{r}')$ is the associated Green's function, that describes the i component of the response at $\underline{r}$ to a point-source force in the j direction at point $\underline{r}'$, in the presence of the sphere S. $\delta C(\delta\rho)$ are the difference between the elastic tensors (densities) of the defect and the medium in which it is embedded.

The DWBA consists of replacing in the integrals of (1) the exact solution u_i by the spherical solution u_i^S, i.e.,

$$u_i^{DWBA}(\underline{r}) = u_i^S(\underline{r}) + \delta\rho\omega^2\int_{\bar{R}} d\underline{r}' g_{im}^S(\underline{r},\underline{r}')u_m^S(\underline{r}') - \delta C_{jklm}\int_{\bar{R}} d\underline{r}' g_{ij,k'}^S(\underline{r},\underline{r}')u_{l,m'}^S(\underline{r}') \quad (2)$$

The solution u^S is known[2] and can be evaluated numerically. However the Green's function g^S is not known; only one component has been explicitly evaluated, and the resulting expressions are rather complex.[3] Therefore last year we studied an intermediate approximation, obtained by replacing g^S in (2) by the infinite Green's function. This approximation is one of a hierarchy of approximations that are discussed below. The main problem in obtaining the DWBA is twofold: to evaluate g^S and to set up the numerical procedure to calculate the integrals.

THE SPHERICAL GREEN'S FUNCTION

To evaluate $g_{ij}(\underline{r},\underline{r}')$ we use the principles of superposition and reciprocity.[4] Our method yields the function for $\underline{r} \to \infty\hat{r}$, which is precisely the one needed in (2), since the point of observation, $\underline{r}$, is assumed to be at infinity for calculation of scattering amplitudes and cross sections.

First note that if the infinite medium Green's function $g^0(\underline{r}',\underline{r})$ can be expanded in terms of plane waves,

$$g_{ij}^0(\underline{r}',\underline{r}) = \sum_\lambda \int d\underline{k} A_j(\underline{r},\underline{k},\lambda)u_i^0(\underline{r}',\underline{k},\lambda) \quad , \quad (3)$$

where $u_i^0(\underline{r}',\underline{k},\lambda)$ are plane wave solutions of the (homogeneous medium) wave equation, the spherical Green's function will be given by

(a) Address after September 1979: Department of Electronics, Weizmann Institute of Science, Rehovot, Israel
(b) Permanent address: Department of Physics, Cornell University, Ithaca, New York

$$g^S_{ij}(\underline{r}',\underline{r}) = \sum_\lambda \int d\underline{k} A_j(\underline{r},\underline{k},\lambda) u^S_i(\underline{r}',\underline{k},\lambda) \quad , \qquad (4)$$

where $u^S_i(\underline{r}',\underline{k},\lambda)$ is the solution of the scattering problem by a sphere, of the incident plane wave $u^0_i(\underline{r}',\underline{k},\lambda)$. (The index λ stands for the various possible polarizations.) Therefore, once the expansion coefficients $A_j(\underline{r},\underline{k},\lambda)$ are known, the spherical Green's function can be constructed, in principle, by superposition of solutions for the incident plane wave scattering problem. In general it is not trivial to find the $A_j(r,k,\lambda)$ needed to expand $g^0_{ij}(\underline{r}',\underline{r})$; however, when the "source" position $\underline{r} \to \infty\hat{r}$, the expansion for the A_j is simple. To see this, note

$$4\pi\rho\omega^2 g^0_{ij}(\underline{r}',\underline{r}) = \frac{\delta_{ij}\beta^2 e^{i\beta R}}{R} - \partial_i\partial_j\left[\frac{e^{i\alpha R}}{R} - \frac{e^{i\beta R}}{R}\right] \qquad (5)$$

with $R = |\underline{r} - \underline{r}'|$, $\partial_j = \partial/\partial r_j$, and $\alpha^2 = \rho\omega^2/(\lambda+2\mu)$, $\beta^2 = \rho\omega^2/\mu$. In the limit $r \to \infty\hat{r}$, this expression becomes

$$4\pi\rho\omega^2 g^0_{ij}(\underline{r}',\underline{r}) = \beta^2 \frac{e^{i\beta r}}{r} e^{-i\beta\hat{r}\cdot\underline{r}'} (\delta_{ij} - \hat{r}_i\hat{r}_j) + \alpha^2 \frac{e^{i\alpha r}}{r} e^{-i\alpha\hat{r}\cdot\underline{r}'} \hat{r}_i\cdot\hat{r}_j \quad . \qquad (6)$$

Introducing now three unit vectors e^λ; $\hat{e}^1 = \hat{r}$, $\hat{e}^2 = \hat{\theta}$, $\hat{e}^3 = \hat{\phi}$, this reads

$$4\pi\rho\omega^2 g^0_{ij}(\underline{r}',\underline{r}\to\infty\hat{r}) = \beta^2 \frac{e^{i\beta r}}{r} e^{-i\beta\hat{r}\cdot\underline{r}'} (\hat{e}^2_j\hat{e}^2_i + \hat{e}^3_j\hat{e}^3_i) + \alpha^2 \frac{e^{i\alpha r}}{r} e^{-i\alpha\hat{r}\cdot\underline{r}'} \hat{e}_j\hat{e}_i \quad . \qquad (7)$$

This expression has the form (3), with only three incident plane waves,

$$\vec{u}^0(\underline{r}',\underline{k},\lambda) = \hat{e}^\lambda e^{-i\gamma(\lambda)\hat{r}\cdot\underline{r}'} \quad , \qquad (8)$$

needed to expand g^0. The coefficients A_j can be read off as given by

$$A_j(\underline{r},\underline{k},\lambda) = \frac{1}{4\pi\rho\omega^2} \hat{e}^\lambda_j \frac{e^{ikr}}{r} k^2\delta[\underline{k} + \gamma(\lambda)\hat{r}] \quad , \qquad (9)$$

where

$$\gamma(1) = \alpha \quad , \quad \gamma(2) = \gamma(3) = \beta \quad . \qquad (10)$$

Finally, in this limit, the spherical Green's function reads

$$4\pi\rho\omega^2 g_{ij}(\underline{r}',\underline{r}\to\infty\hat{r}) = \sum_\lambda \hat{e}^\lambda_j \frac{e^{i\gamma(\lambda)r}}{r} \gamma(\lambda)^2 u^S_i(\underline{r}',-\gamma(\lambda)\hat{r},\lambda) \qquad (11)$$

where $u^S_i(\underline{r}',-\gamma(\lambda)\hat{r},\lambda)$ is the solution for scattering by a sphere of a plane wave with polarization λ, wavevector $\gamma(\lambda)$, incident in the $-\hat{r}$ direction, evaluated at point $\underline{r}'$.

Inspecting Eq. (2) we note that in order to evaluate $u^{DWBA}(r)$ in the far field, i.e., $\underline{r} \to \infty$, we need g^S with the point of observation at ∞. To obtain this function, we use reciprocity,[4] e.g.,

$$g_{ij}(\underline{a},\underline{b}) = g_{ji}(\underline{b},\underline{a}) \quad , \qquad (12)$$

to get

$$g^S_{ji}(\underline{r}\to\infty,\underline{r}') = \frac{1}{4\pi\rho\omega^2} \sum_\lambda \hat{e}^\lambda_j \frac{e^{i\gamma(\lambda)r}}{r} \gamma(\lambda)^2 \cdot u^S_i(\underline{r}',-\gamma(\lambda)\hat{r},\lambda) \quad . \qquad (13)$$

THE DISTORTED WAVE BORN APPROXIMATION-- FAR FIELD AMPLITUDES

In the far field limit, the scattered wave has the form

$$\vec{u}^{DWBA} = \sum_\lambda \hat{e}^\lambda A(\lambda) e^{i\gamma(\lambda)r}/r \quad . \qquad (14)$$

The solution of the scattering problem by a sphere, $\vec{u}^S$, has this asymptotic form, and by inspection of Eq. (13), so does the spherical Green's function, and therefore, $\vec{u}^{DWBA}$.

To obtain closed form expressions for $\vec{u}^{DWBA}$, we substitute (13) in Eq. (2). To make the notation uniform, we denote the scattered solution that corresponds to the physical incident wave as $u^S[\underline{r},-\gamma(\mu)\hat{r}_0,\lambda_0]$ where $-\hat{r}_0$ is the direction of incidence, and λ_0 the polarization of the incident wave. Substitution of (13) in (2) yields, for $\underline{r} \to \infty\hat{r}$,

$$\vec{u}^{DWBA}(\underline{r},-\gamma(\lambda_0)\hat{r}_0,\lambda_0) = \vec{u}^S(\underline{r},-\gamma(\lambda_0)\hat{r}_0,\lambda_0) + \sum_\lambda \hat{e}^\lambda \gamma(\lambda)^2 \frac{e^{i\gamma(\lambda)r}}{r} [D_1 + D_2 + D_3] \quad , \qquad (15)$$

where

$$D_1 = \frac{\delta\rho}{4\pi\rho} \int_{\bar{R}} d\underline{r}' u^S_m(\underline{r}',-\gamma(\lambda)\hat{r},\lambda) u^S_m(\underline{r}',-\gamma(\lambda_0)\hat{r}_0,\lambda_0)$$

$$D_2 = -\frac{\delta\lambda}{4\pi\rho\omega^2} \int_{\bar{R}} d\underline{r}' u^S_{m,m'}(r',-\gamma(\lambda)\hat{r},\lambda) u^S_{1,1'}(\underline{r}',-\gamma(\lambda_0)\hat{r}_0,\lambda_0$$

$$D_3 = \frac{-2\delta\mu}{4\pi\rho\omega^2} \int_{\bar{R}} d\underline{r}' \varepsilon^S_{jk}(\underline{r}',-\gamma(\lambda)\hat{r},\lambda) \varepsilon^S_{jk}(\underline{r}',-\gamma(\lambda_0)\hat{r}_0,\lambda_0) \qquad (16)$$

with

$$u_{i,j'} = \partial u_i/\partial r'_j$$

and

$$\varepsilon_{jk} = \frac{1}{2}[u_{j,k'} + u_{k,j'}] \quad .$$

Note that the constants D depend on the incident an scattered directions $\hat{r}_0$ and $\hat{r}$, as well as on the polarizations of the incident and scattered fields, λ_0 and λ.

We have numerically evaluated the longitudinal cattered fields for incident longitudinal waves. or this problem only the $\hat{r} = \hat{e}'$ component enters, nd therefore, only the spherical solutions for an ncident longitudinal wave are needed.

The results are given below.

RESULTS

We first performed various checks on our procedure. In particular, we used g^S in the exact integral equation (1). For the case where the defect R s a sphere of radius a_2, represented as a sphere of adius $a_1 < a_2$ and a remainder volume, the exact olution inside R can be calculated, inserted in 1), and the result is compared with the far field olution for R. We obtained agreement, with accuracy that characterizes our numerical integration rocedure (~1%). Next, we turned to study the accuracy of the DWBA, by calculating the scattered ield from a sphere R using (15)-(16). This was one for Al spheres in Ti and for cavities in Ti; he ratios of the radii of the actual sphere R and he inner sphere S was $a_2/a_1 = 1.2$ and $a_2/a_1 = 2$. ote that in the former case the volume "perturbaion" is $\bar{R}/S \tilde{=} 70\%$, while for $a_2/a_1 = 2$ it is $\bar{R}/S = 00\%$.

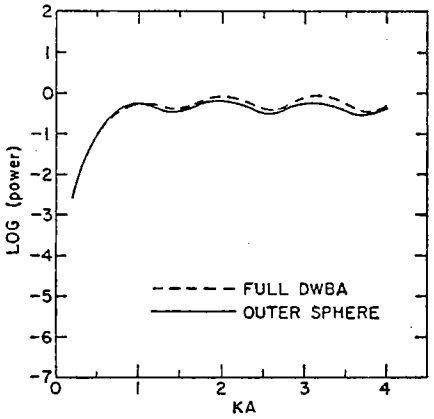

ig. 2. Spherical cavity in Ti: Longitudinal backscattered wave, log (power) versus ka for a ratio of radii of 6/5.

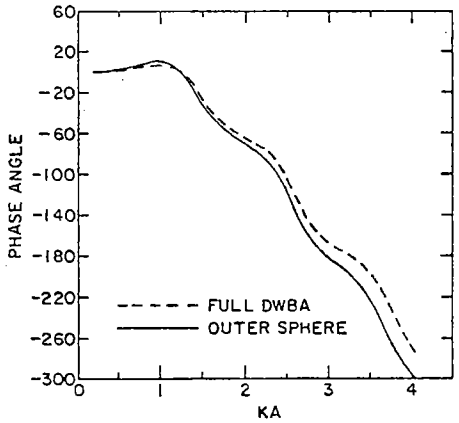

Fig. 3. Spherical cavity in Ti: Longitudinal backscattered wave, phase angle versus ka for a ratio of radii of 6/5.

For the sake of comparison, we also show the results of the intermediate approximation (i.e., g^S replaced by g^0 in Eq. (2)).

The results of these checks are shown in Figs. (2) - (8). In general, the DWBA reproduces fairly well the exact results for the frequency and angular dependence of both power and phase. For the large perturbation $a_2/a_1 = 2$, the DWBA breaks down, for Al in Ti, at around ka > 3.5. However, for $a_2/a_1 = 1.2$ the DWBA is good, even for a strong scatterer like a cavity, for a wide range of ka.

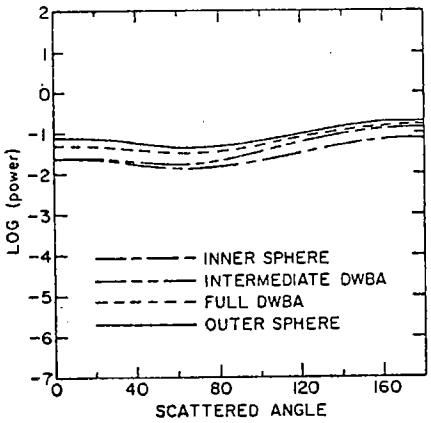

Fig. 4. Spherical cavity in Ti: Longitudinal wave, log (power) versus θ for ka = .6 and ratio of radii of 6/5.

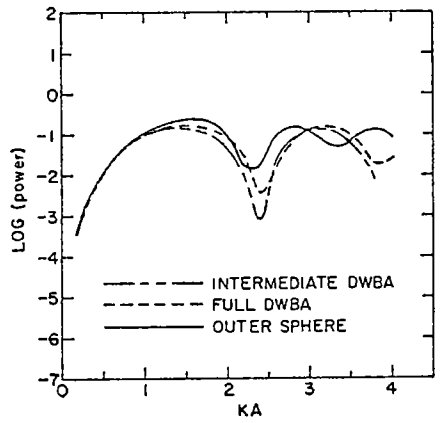

Fig. 5. Al sphere in Ti: Longitudinal backscattered wave, log (power) versus ka for a ratio of radii of 2.

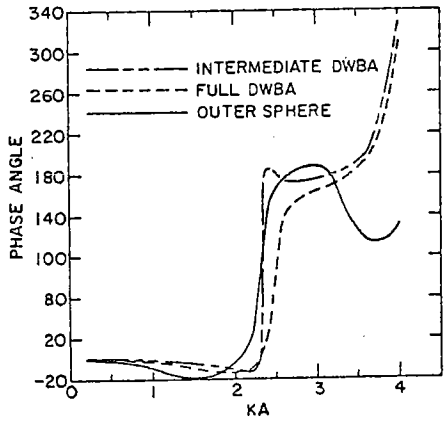

Fig. 6. Al sphere in Ti: Longitudinal backscattered wave, phase angle versus ka for a ratio of radii of 2.

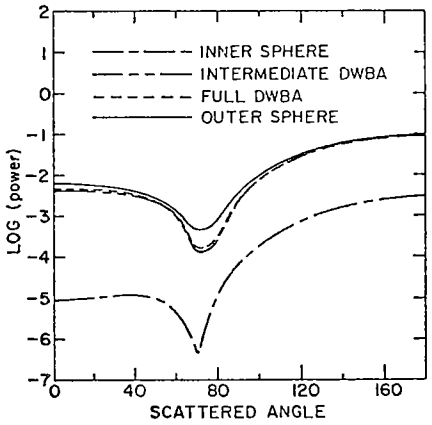

Fig. 7. Al sphere in Ti: Longitudinal wave, log (power) versus θ for ka = 1 and ratio of radii of 2.

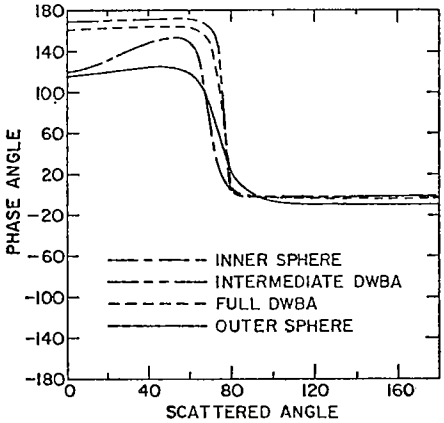

Fig. 8. Al sphere in Ti: Longitudinal wave, phase angle versus θ for ka = 1 and ratio of radii of 2.

Next, we turn to study a nonspherical defect, shown in Fig. (9). The defect is a spherical cavity of diameter 800μ, to which a hemisphere cavity of diameter 400μ has been added. We will refer to the hemisphere as the "bubble"; it represents a deviation of size b from a simple shaped smooth cavity of characteristic size a. The questions we addressed are the following:

(1) At what frequencies (e.g., values of kb) is the bubble observable?

(2) At what angles of incidence and scattering is its effect most pronounced?

To answer these questions, we present, first, Figs. (10) - (12), which show the backscattered power vs. ka for three incident directions. These figures compare the scattering by the large sphere to that of the nonspherical defect. We find that experimentally observable differences (i.e., ∿3db) show up when ka ≳ 1.5 (i.e., kb ≳ .75). We also note that the largest deviation is obtained for $\theta_0 = 180^0$ (see Fig. 12), i.e., when the bubble is directly illuminated.

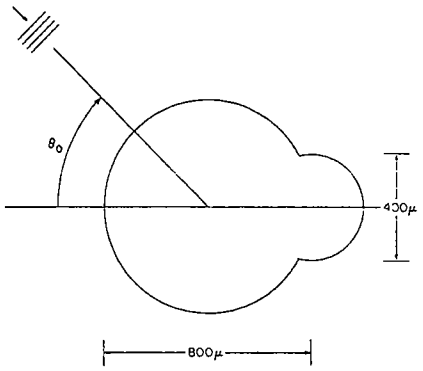

Fig. 9. Bubble defect: Direction of incidence is denoted by θ_0.

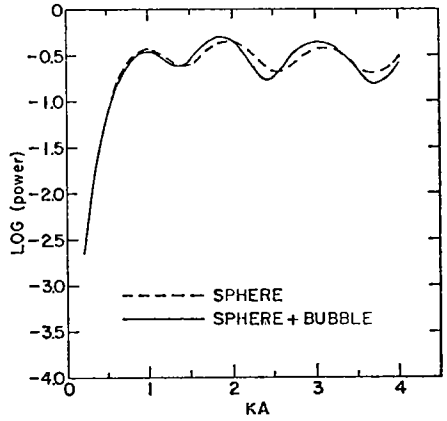

Fig. 10. Bubble defect in Ti: Longitudinal backscattered power, log (power) versus ka for shadowed incidence, $\theta_0 = 0$.

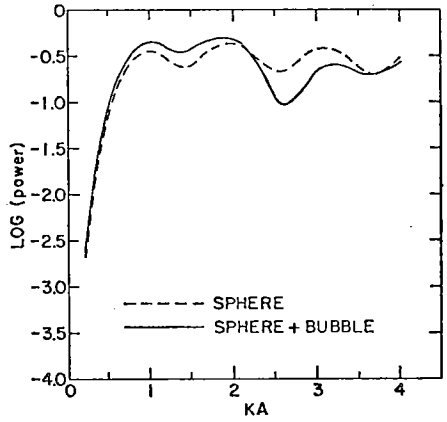

Fig. 11. Bubble defect in Ti: Longitudinal backscattered wave, log (power) versus ka for incidence direction $\theta_0 = 90$.

The frequency spectrum is modulated with about the same periodicity as that of a sphere, but a modulation with longer periodicity (in k) is superimposed. While for the sphere the first three peaks are of approximately equal amplitude, with the bubble present the amplitudes decrease in magnitude (for the first three peaks).

Turning now to angular distribution of power the sequence of Figs. 13-15 shows polar plots of power vs. scattering angle for three directions of incidence and ka values of 1 and 2.

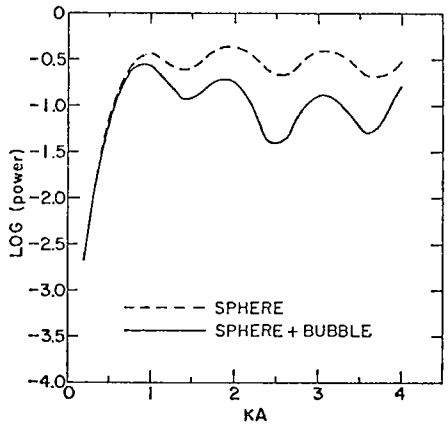

Fig. 12. Bubble defect in Ti: Longitudinal backscattered wave, log (power) versus ka for direct incidence, $\theta_0 = 180$.

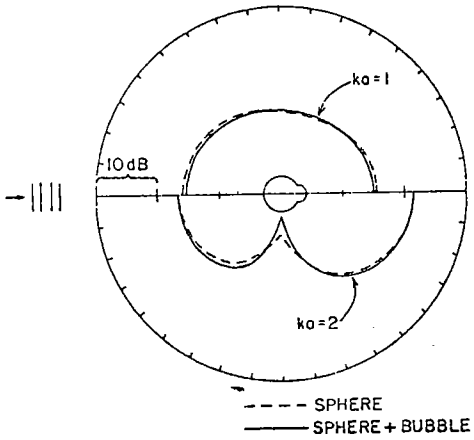

Fig. 13. Bubble defect in Ti: Longitudinal wave, log (power) versus θ for shadowed incidence, ka = 1,2.

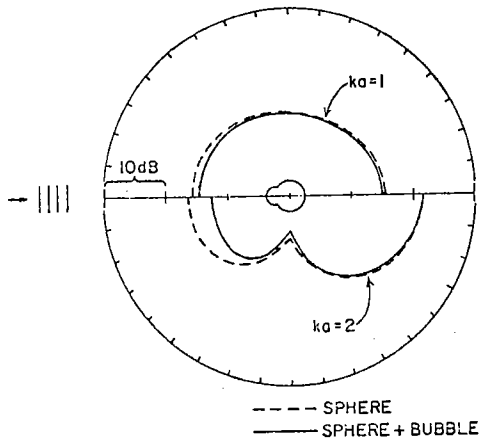

Fig. 14. Bubble defect in Ti: Longitudinal wave, log (power) versus θ for direct incidence, ka = 1,2.

Again we note that the effect of the bubble is observable at ka = 2, and not at ka = 1. Also, the largest effect is obtained for $\theta_0 = 180$ (i.e., direct illumination), and even then the best results are obtained for backscattering.

It is of interest to observe the loss of symmetry of the scattered power, caused by the presence of the bubble. Figs. 15 and 16 show this effect; in particular, the results of Fig. 16, with incidence at $\theta_0 = 90$ and scattering at $\theta = 135^0$ have been verified experimentally.[5]

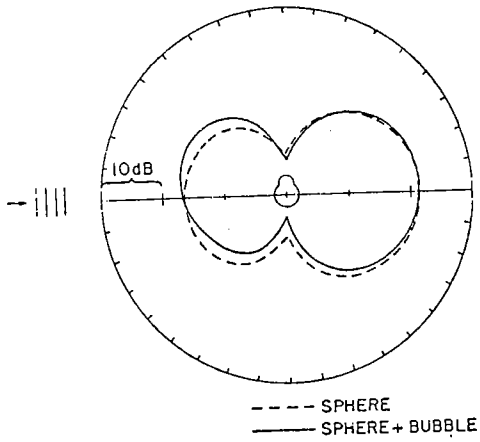

Fig. 15. Bubble defect in Ti: Longitudinal wave, log (power) versus scattering angle θ for incident direction $\theta_0 = 90$, ka = 2; the scattered direction is in the plane defined by the incident direction and the symmetry axis of the scatterer.

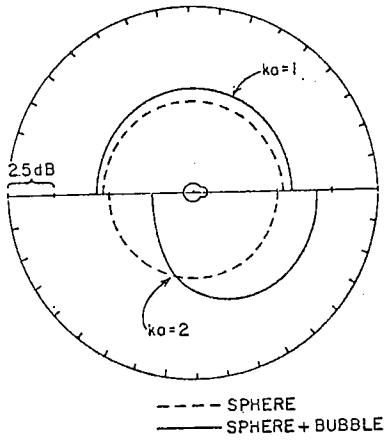

Fig. 16. Bubble defect in Ti: Longitudinal wave, log (power) versus azimuthal angle ϕ for incidence direction $\theta_0 = 90$, scattering angle $\theta = 135$, and ka = 1,2.

SUMMARY

The DWBA gives analytically simple forms for the scattering of elastic waves by defects of quite general shape. Our numerical studies indicate that the approximation yields reliable frequency dependence and phase information. Initial comparisons with experiment were most encouraging.

We plan to extend this work to obtain the scattered shear waves, and to use the procedure to test inversion procedures[6] and the concept of defect representation by effective ellipsoids.[7]

ACKNOWLEDGMENTS

This research was sponsored by the Center for Advanced NDE, operated by the Science Center, Rockwell International, for the Advanced Research Projects Agency and the Air Force Materials Laboratory under contract F33615-74-C-5180. We thank C. Kirschbaum and B. Yanoff for programming assistance.

REFERENCES

1. K.E. Newman and E. Domany, Proceedings of the ARPA/AFML Review of Progress in Quantitative NDE, ed. D.O. Thompson, AFML-TR-78-205, p. 404 (1978).

2. C.F. Ying and R. Truell, J. Appl. Phys. 27, 1086 (1956); G. Johnson and R. Truell, J. Appl. Phys. 36, 3466 (1965).

3. K.E. Newman, C.K. Lam and E. Domany; The Elastodynamics Green's Function for a Spherical Defect, submitted for publication.

4. J. E. Gubernatis, unpublished.

5. B. R. Tittmann, these proceedings.

6. J. H. Rose, these proceedings.

7. A. N. Mucciardi, these proceedings.

SUMMARY DISCUSSION
(Eytan Domany)

John Richardson (Science Center): When you talk about deviation from a sphere, is it the original sphere you have drawn or slightly larger sphere that has the same volume or something like that, the perturbed --

Eytan Domany: I just meant from the original sphere from which the sensor is attached. That's what we compare.

Jim Krumhansl (Cornell University): If I were to intuitively extrapolate what you say to the issue of whether some kind of join which was just bad glue and had fluctuations on a scale, you know, like a tenth of the radius, I would really have to go to the K equal 10 or something like that to find that.

Eytan Domany: If you characterize the deviation from the structure you want to look at, which in this case would be the small ripples, as having the characteristic length of B, then KB should be about one. That's the right measure. I think the thing that should be done is to extend the comparison experiment to see whether the phase angle you can get out of this is borne out by the approximate theory.

Jim Rose (University of Michigan): Your perturbation seems to be delta DOD, or a change in volume. Does that mean for small changes in volume you can do sharp corners or that kind of thing?

Eytan Domany: That's a good question. The question is what do you mean by "can do"? You can do anything with born approximations. I can fully transform this microphone. The question is when you do that whether it makes any sense. So, in the same way here, one has to integrate a deviation from the sphere, so you have to have sharp corners just to integrate, or a volume that has sharp corners. Now, the physics of sharp corners is mainly, as I understand it, singularities in the ray of physical sphere near those sharp corners. Those will not be picked up by this method. What you will pick up is that you take some smooth field and you integrate it over an object that has sharp corners. As far as that effect goes, it will be in there. But the real physics of physical displacement and stray field, which is singular as a result of having those sharp corners, that's not going to be in there. And I sort of feel if it's not going to be in any of the approximations that have been discussed, I think that's moot. You're not having either, because they're also, unless you view the singularity effect that Bill was talking about. Did I answer your question?

Jim Rose: You answered the question.

# #